Journal of Solid State Chemistry **163,** 113–120 (2002)
doi:10.1006/jssc.2001.9379, available online at http://www.idealibrary.com on IDEAL®

# Homoatomic Clustering in the Intermediate Valence Compounds $Yb_{1-y}Al_{3-x}Si_x$ and $Yb_{1-y}Al_{3-x}Ge_x$

Jing-Tai Zhao,*,† Walter Schnelle,* and Yuri Grin*,[1]

*Max-Planck-Institut für Chemische Physik fester Stoffe, Nöthnitzer Strasse 40, 01187 Dresden, Germany; and †College of Chemistry and Chemical Engineering, Xiamen University, Xiamen 361005, People's Republic of China

Received March 27, 2001; in revised form August 24, 2001; accepted August 24, 2001

**Two new phases, $Yb_{1-x}Al_{3-x}Si_x$ and $Yb_{1-y}Al_{3-x}Ge_x$, were found by systematic investigations of the according ternary systems. The crystal structures of $Yb_{1-y}Al_{2.8}Si_{0.2}$ and $Yb_{1-y}Al_{2.8}Ge_{0.2}$ (defect HT-$PuAl_3$ type) were studied by X-ray powder methods (Cu$K\alpha_1$ radiation, $\lambda = 1.54056$ Å, hexagonal system, space group $P6_3/mmc$ (No. 194), $a = 6.009(1)$ and $6.015(1)$ Å, $c = 14.199(2)$ and $14.241(5)$ Å, $V = 444.0(2)$ and $446.2(3)$ Å$^3$, 93 and 92 reflections, and 8200 and 8000 profile points for silicide and germanide, respectively). Full profile refinements with 11 and 13 structural parameters resulted in $R_I = 0.049$ and 0.054, and $R_p = 0.088$ and 0.104, respectively. The ternary structures are distorted closest packings in comparison with the binary $YbAl_3$ compound with $AuCu_3$-type structure. They are characterized by the formation of $Al_3$-, $Si_3$-, and $Ge_3$-homoatomic clusters and aluminum networks. Magnetization measurements show that both the silicide and germanide are valence fluctuation compounds with enhanced electronic density of states at the Fermi level similar to the binary $YbAl_3$. The characteristic maximum of the magnetic susceptibility increases from $\approx 120$ K for $YbAl_3$ to $\approx 140$ K for $Yb_{1-y}Al_{2.8}Si_{0.2}$or $Yb_{1-y}Al_{2.8}Ge_{0.2}$ and further to $\approx 150$ K for $Yb_{1-y}Al_{2.75}Si_{0.25}$. The S-shape of the electrical resistivity curves is also characteristic of valence fluctuations.** 

***Key Words:*** **intermetallic compounds; intermediate valence; ytterbium; aluminum; silicon; germanium; homoatomic clustering; magnetic susceptibility; resistivity.**

## INTRODUCTION

Compounds containing the rare earth element ytterbium show valence instabilities as a function of temperature and/or composition (1,2). The intermetallic compound $YbAl_3$ with the $AuCu_3$-type structure has been investigated for many years for its interesting transport, magnetic, and thermodynamic properties. It was classified as an intermediate valence system, with almost trivalent ions at high temperature (3–6). In the previous systematic studies of the ternary systems of Yb with two main group elements, only two ternary compounds were reported in the Yb–Al–Ge system (7, 8). A few new compounds were characterized recently: $YbAl_2Si_2$ (9, 10), $Yb_2AlSi_2$ (11), and $Yb_2AlGe_3$ (12). Here, we report on two new ternary compounds in the Yb–Al–Ge(Si) systems, which are closely related to $YbAl_3$.

## EXPERIMENTAL

### *Synthesis*

The samples of $YbAl_{3-x}Si_x$ ($x = 0.05, 0.15, 0.20, 0.25, 0.5$) and $YbAl_{3-x}Ge_x$ ($x = 0.1, 0.15, 0.20, 0.25, 0.40, 0.60, 0.80$) were synthesized by high-frequency (HF) induction melting of pure elements (Yb 99.9%, Al 99.999%, Si 99.9999%, Ge 99.9999%) in glassy graphite crucibles. Ytterbium was distilled prior to use. The aluminum wire ($\varnothing = 0.5$ mm), silicon, and germanium lumps were weighed in air, while all the operations involving ytterbium were done inside an argon-filled glove box. Great care was taken in increasing the HF power during the melting to prevent violent reactions and evaporation of the volatile metals. The melting weight losses were less than 0.5%. The bulk samples, although normally sticking to the crucible walls due to negative surface tension of the liquid alloys, can be separated by cutting off the crucible since a clear border between the sample and crucible exists so that severe carbon diffusion at elevated temperature is not expected. The carbon content of the final annealed samples was checked by chemical analysis. The sample pieces were wrapped in molybdenum foil and sealed into argon-filled (400 mbar) quartz glass tubes after several refillings and evacuations ($< 10^{-5}$ mbar). The tubes were then slowly heated to 800°C at a rate of about 100°C/h. After being held at 800°C for 24 h, the temperature was decreased to 600°C within 5 h. The samples were then

[1]To whom correspondence should be addressed. E-mail: grin@cpfs.mpg.de. Fax: + 49-351-4646 4002.



0022-4596/02 $35.00

annealed at 600°C for 10 days and finally quenched in cold water. During annealing the samples did not attack the molybdenum foil; only a slight metallic tinge was observed on some parts of the inner surface of the quartz glass tubes, presumably caused by evaporation of the components.

### *Structure Characterization*

To prevent the reaction of the samples with oxygen and moisture, the powder samples used for X-ray diffraction (XRD) were prepared inside an argon-filled glove box in capillaries or were protected by Kapton film. Refinement of the unit cell parameters was done from powder data using Si as an internal standard ($a = 5.4305$ Å). The structures of $Yb_{1-y}Al_{2.8}Si_{0.2}$ and $Yb_{1-y}Al_{2.8}Ge_{0.2}$ were refined from powder XRD data by using the CSD program (13).

### *Property Measurements*

The magnetic properties were measured using a SQUID magnetometer (MPMS-XL7, Quantum Design). The electrical conductivity was investigated by a conventional four-probe dc method.

## RESULTS AND DISCUSSION

Introduction of the tetrel (i.e., germanium) into the binary $YbAl_3$ compound first leads to a slight increase of the formula unit volume of the $YbAl_{3-x}Ge_x$ phase with the cubic $AuCu_3$ structure ($x < 0.1$, Table 1), in contrast to the atomic radius ratio ($r_{Al} = 1.431$ Å, $r_{Ge} = 1.225$ Å). Further increase of the germanium concentration ($x = 0.15$) causes a change of the structure from $AuCu_3$-type to HT-$PuAl_3$-type (HT, high-temperature modification), accompanied by a slight increase of the formula unit volume. The formula unit volume values for the phases with the HT-$PuAl_3$-type structure in the multi phase samples with $x < 0.2$ and $x > 0.2$ are only slightly different (within a $4\sigma$ error range). Furthermore, the values for the samples with $x \geq 0.2$ are almost equal (within a $2\sigma$ error range). By considering that the sample with $x = 0.15$ is already a multiphase one, we conclude that the $Yb_{1-y}Al_{3-x}Ge_x$ phase with the HT-$PuAl_3$ structure has a narrow homogeneity range around $x = 0.2$.

**TABLE 1**
**Unit Cell Parameters for the $Yb_{1-x}Al_{3-x}Si_x$ and $Yb_{1-y}Al_{3-x}Ge_x$ Phases**

| Sample | Structure type | $a$ (Å) | $c$ (Å) | $V$ (Å$^3$)[a] | Remark |
|---|---|---|---|---|---|
| $YbAl_3$ | $AuCu_3$ | 4.200 | | 74.0 | [5] |
| $Yb_{1-y}Al_{3-x}Ge_x$ ($x < 0.1$) | $AuCu_3$ | 4.2030(1) | | 74.25(1) | [b] |
| $Yb_{1-y}Al_{2.85}Ge_{0.15}$ | HT-$PuAl_3$ | 6.0146(7) | 14.285(3) | 74.58(3) | [b] |
| $Yb_{1-y}Al_{2.8}Ge_{0.2}$ | HT-$PuAl_3$ | 6.015(1) | 14.241(5) | 74.37(5) | [c] |
| $Yb_{1-y}Al_{2.6}Ge_{0.4}$ | HT-$PuAl_3$ | 6.0165(9) | 14.230(4) | 74.35(5) | [b] |
| $Yb_{1-y}Al_{2.4}Ge_{0.6}$ | HT-$PuAl_3$ | 6.018(1) | 14.235(4) | 74.42(5) | [b] |
| $Yb_{1-y}Al_{2.85}Si_{0.15}$ | HT-$PuAl_3$ | 6.0112(7) | 14.234(2) | 74.23(3) | [b] |
| $Yb_{1-y}Al_{2.8}Si_{0.2}$ | HT-$PuAl_3$ | 6.009(1) | 14.199(2) | 74.00(3) | [c] |
| $Yb_{1-y}Al_{2.75}Si_{0.25}$ | HT-$PuAl_3$ | 6.0101(6) | 14.170(2) | 73.88(3) | [c] |
| $Yb_{1-y}Al_{2.5}Si_{0.5}$ | HT-$PuAl_3$ | 6.0119(7) | 14.145(2) | 73.78(3) | [b] |

[a] $V$, volume per formula unit $YbE_3$.
[b] Multiphase sample.
[c] Single-phase sample.

**TABLE 2**
**Crystallographic Data for $Yb_{1-y}Al_{2.8}Si_{0.2}$ and $Yb_{1-y}Al_{2.8}Ge_{0.2}$**

| | $Yb_{1-y}Al_{2.8}Si_{0.2}$ | $Yb_{1-y}Al_{2.8}Ge_{0.2}$ |
|---|---|---|
| Structure type | HT-$PuAl_3$ | |
| Space group | $P6_3/mmc$ (No. 194) | |
| $a$ (Å) | 6.009(1) | 6.015(1) |
| $c$ (Å) | 14.199(2) | 14.241(5) |
| $V$ (Å$^3$) | 444.0(2) | 446.2(3) |
| $Z$ | 6 | |
| $D_x$ (g cm$^{-3}$) | 5.704 | 5.884 |
| $\mu$ (cm$^{-1}$) | 656.44 | 669.4 |
| Radiation | Cu $K\alpha_1$, $\lambda = 1.54056$ Å | |
| Diffractometer | STOE STADI MP | |
| No. of points | 8200 | 8000 |
| No. of reflections | 93 | 92 |
| Mode of refinement | Full profile | |
| No. of parameters | 11 | 13 |
| $2\theta$ and $(\sin\theta/\lambda)_{max}$ | 99.10, 0.494 | 89.15, 0.456 |
| $R_I$, $R_p$, $R_{DBW}$ | 0.049, 0.088, 0.079 | 0.054, 0.104, 0.087 |

The situation for the silicide is somewhat different from that for the germanide. The formula unit volume for the $Yb_{1-y}Al_{3-x}Si_x$ phase (HT-$PuAl_3$ type of structure) with $x = 0.15$ is 74.23 Å$^3$ and subsequently drops with a difference of 0.45 Å$^3$ (larger than $15\sigma$ error range) for the sample with $x = 0.5$. From these observations, the single-phase region for the HT-$PuAl_3$ type of structure lies approximately in the range $0.15 < x < 0.3$. This larger homogeneity range is consistent with the XRD powder patterns observed in single-phase materials for samples with $x = 0.2$ and $x = 0.25$.

The crystal structure of $Yb_{1-y}Al_{2.8}Ge_{0.2}$ was refined by the full profile method. Crystallographic data and experimental details are presented in Table 2, and observed and calculated X-ray powder patterns together with their difference plot are shown in Fig. 1. The primary refinement with isotropic atomic displacement ($R_I = 0.057$) made possible to distinguish the occupancy of the Al1 and Al2 positions: the germanium atoms obviously prefer to locate on the Al1 site (see Table 3). The resulting interatomic distance ($d$(Al1–Al1) = 2.70 Å) is remarkably shorter than the Al–Al contacts in the binary $YbAl_3$ structure (2.97 Å) and hard to interpret in terms of atomic radii ($2r_{Al} = 2.862$ Å,

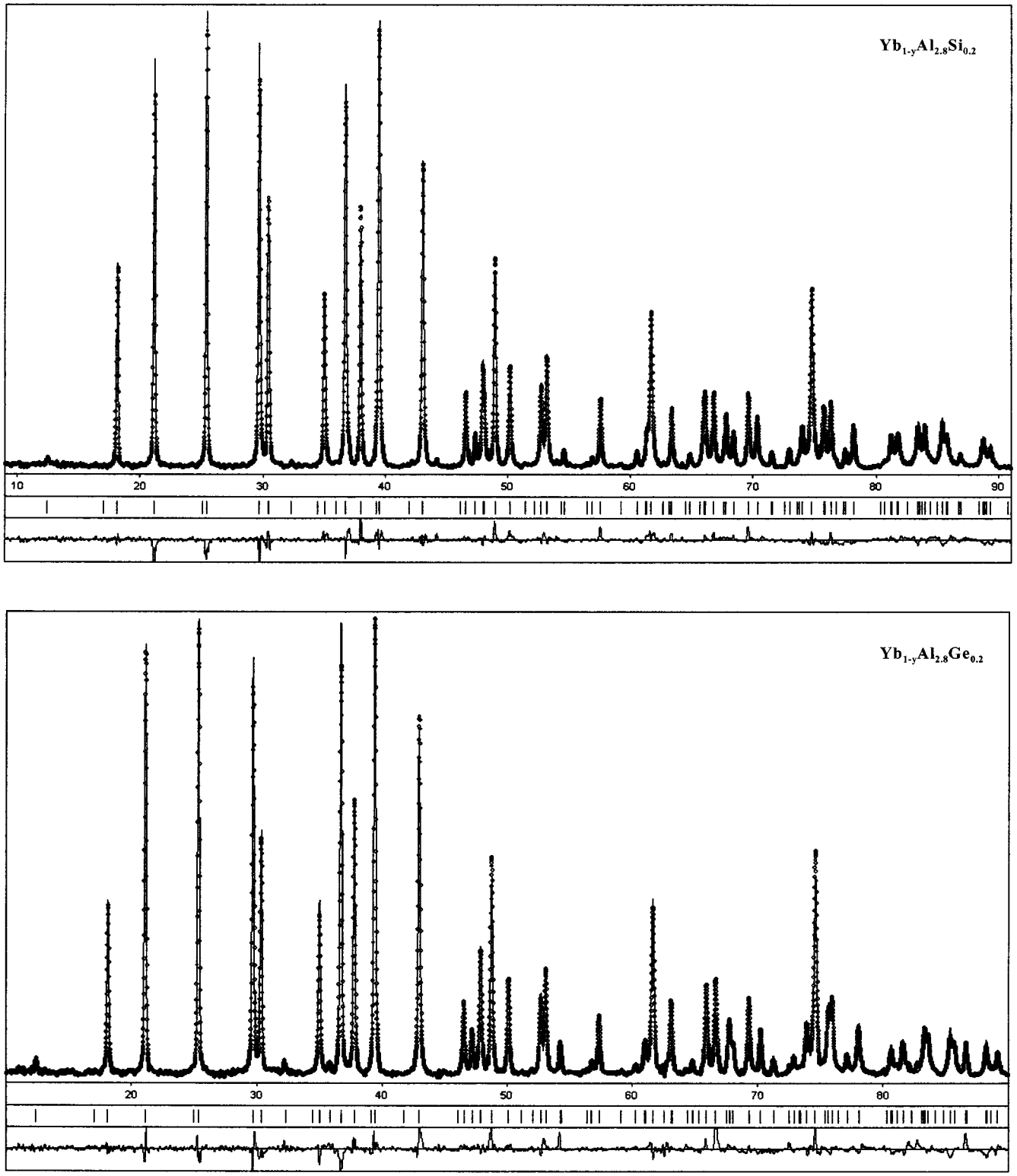


**FIG. 1.** Observed and calculated XRD powder patterns together with their difference plots for $Yb_{1-y}Al_{2.8}Si_{0.2}$ (upper panel) and $Yb_{1-y}Al_{2.8}Ge_{0.2}$ (lower panel).

**TABLE 3**
**Atomic Positional and Displacement Parameters for $Yb_{1-y}Al_{2.8}Ge_{0.2}$**

| Atom | Site | SOF | $x$ | $y$ | $z$ | $U_{iso}$ (in Å$^2$) |
|---|---|---|---|---|---|---|
| Yb1 | 2*b* | 1 | 0 | 0 | $\frac{1}{4}$ | 0.0047(4) |
| Yb2 | 4*f* | 0.948(3) | $\frac{1}{3}$ | $\frac{2}{3}$ | 0.08977(8) | 0.0062(3) |
| Al1 | 6*h* | 0.83(2) | 0.510(1) | $2x-1$ | $\frac{1}{4}$ | 0.008(1) |
| Ge1 | | 0.17 | 0.530(1) | $2x-1$ | $\frac{1}{4}$ | 0.008 |
| Al2 | 12*k* | 0.985(1) | 0.8310(3) | $2x-1$ | 0.0833(2) | 0.0082(8) |
| Ge2 | | 0.015 | 0.8310 | $2x-1$ | 0.0833 | 0.0082 |

$2r_{Ge} = 2.45$ Å). The remaining Al2–Al2 and Al2–Al1 contacts are on the level of aluminum–aluminum distances in the binary compound (see Table 4). The attempt to refine the Al1 position in anisotropic approximation led to a very distorted ellipsoid with $\mathbf{B}_{11} = 0.6(1)$, $\mathbf{B}_{22} = 1.3(2)$, and $\mathbf{B}_{33} = 0.2(2)$. The experimental electron density in this region seems not to be described by only one ellipsoid. The electron density map at the *ab*-plane with $z = 0.25$ confirms considerable irregularity of the electron density around the Al1 position (Fig. 2). The aluminum and germanium parts were then calculated with different coordinates (split model). A subsequent refinement was successful ($R_I = 0.054$). The final structure model contains an aluminum position (occupancy 0.83) with $d$(Al–Al) = 2.827 Å and an alternative germanium position (occupancy 0.17) with $d$(Ge–Ge) = 2.47 Å, avoiding the discrepancy mentioned above. Both atom sorts form the $E_3$ ($E$ = Al, Ge) groups with short intercontacts. The full accordance of the interatomic distances in the $E_3$ triangles with the atomic radii is consistent with the interpretation that, in each case, they contain covalently bonded atoms of one kind only. This obviously follows the tendency of the main group elements to form homoatomic clusters in electron-deficient systems. However, this effect is usually not observed by concentrations of clustering atoms as small as Si or Ge in $Yb_{1-y}Al_{3-x}Si_x$ and $Yb_{1-y}Al_{3-x}Ge_x$. The $Al_3$ and $Ge_3$ "clusters" are distributed statistically with respect to the occupancy factors. One of the ytterbium sites (Yb2) in the germanide reveals significant defects (refined occupancy 0.948, see below).

**TABLE 4**
**Interatomic Distances (in Å) for $Yb_{1-y}Al_{2.8}Si_{0.2}$ and $Yb_{1-y}Al_{2.8}Ge_{0.2}$**

| | $Yb_{1-y}Al_{2.8}Si_{0.2}$ | | | | $Yb_{1-y}Al_{2.8}Ge_{0.2}$ | | | |
|---|---|---|---|---|---|---|---|---|
| Yb1 | — 6 | Al2 | 2.964(2) | Yb1 | — 6 | Al2 | 2.956(3) |
| | — 6 | Al1 | 3.011(2) | | — 6 | Al1 | 3.01(2) |
| | | Si1 | 3.03(3) | | | Ge1 | 3.024(7) |
| | — 6 | Yb2 | 4.131(1) | | — 6 | Yb2 | 4.155(1) |
| Yb2 | — 3 | Al1 | 2.958(3) | Yb2 | — 3 | Al1 | 2.932(4) |
| | | Si1 | 3.09(2) | | | Ge1 | 3.067(9) |
| | — 3 | Al2 | 3.006(3) | | — 3 | Al2 | 3.001(3) |
| | — 6 | Al2 | 3.009(2) | | — 6 | Al2 | 3.009(2) |
| | — 3 | Yb1 | 4.131(1) | | — 3 | Yb1 | 4.155(1) |
| | — 3 | Yb2 | 4.345(1) | | — 3 | Yb2 | 4.312(1) |
| Al1 | — 2 | Al1 | 2.666(3) | Al1 | — 2 | Al1 | 2.827(9) |
| | | Si1 | 2.50(2) | | | Ge1 | 2.65(1) |
| | — 4 | Al2 | 2.904(4) | | — 4 | Al2 | 2.905(5) |
| | — 2 | Yb2 | 2.958(3) | | — 2 | Yb2 | 2.932(4) |
| | — 2 | Yb1 | 3.011(4) | | — 2 | Yb1 | 3.009(8) |
| | — 2 | Al1 | 3.343(6) | | — 2 | Al1 | 3.189(9) |
| | | Si1 | 3.51(2) | | | Ge1 | 3.37(1) |
| Si1 | — 2 | Al1 | 2.50(2) | Ge1 | — 2 | Al1 | 2.65(1) |
| | | Si1 | 2.34(3) | | | Ge1 | 2.47(2) |
| | — 4 | Al2 | 2.87(1) | | — 4 | Al2 | 2.856(9) |
| | — 2 | Yb2 | 3.03(3) | | — 2 | Yb2 | 3.067(8) |
| | — 2 | Yb1 | 3.09(2) | | — 2 | Yb1 | 3.01(2) |
| | — 2 | Al1 | 3.51(2) | | — 2 | Al1 | 3.37(1) |
| | | Si1 | 3.67(3) | | | Ge1 | 3.55(2) |
| Al2 | — 2 | Al1 | 2.904(4) | Al2 | — 2 | Al1 | 2.905(2) |
| | | Si1 | 2.87(1) | | | Ge1 | 2.856(5) |
| | — 2 | Al2 | 2.891(3) | | — 2 | Al2 | 2.955(4) |
| | — | Yb1 | 2.964(2) | | — | Yb1 | 2.956(3) |
| | — 2 | Al2 | 2.990(2) | | — 2 | Al2 | 2.965(3) |
| | — | Yb2 | 3.006(3) | | — | Yb2 | 3.001(3) |
| | — 2 | Yb2 | 3.009(2) | | — 2 | Yb2 | 3.009(3) |
| | — 2 | Al2 | 3.020(2) | | — 2 | Al2 | 3.050(3) |

Refinement of the $Yb_{1-y}Al_{2.8}Si_{0.2}$ structure led to similar results ($\mathbf{B}_{11} \approx \mathbf{B}_{22} \gg \mathbf{B}_{33}$ for the Al1 position). Observed and calculated X-ray powder patterns together with their difference plot are also shown in Fig. 1. The crystallographic data are listed in Table 2, the atomic positional and displacement parameters are shown in Table 5, and interatomic distances are presented in Table 4.

The composition of the single-phase $Yb_{1-y}Al_{2.8}Ge_{0.2}$ sample was proven by chemical analysis (ICP method). The result of the analysis—$Yb_{0.96(1)}Al_{2.81(4)}Ge_{0.19(1)}$—corresponds well with the crystallographic data, confirming the nonfull occupancy of the Yb2 position and being consistent with weight losses during the synthesis.

It is worthwhile to check the carbon content diffused into the samples since graphite crucibles were used during the synthesis. Although the samples can be separated along the clear border between the samples and the wall of the crucible, diffusion of some carbon cannot be excluded at elevated temperature. The carbon contents of the final annealed samples were found by chemical analysis to be $< 0.9$ at.% for the silicide and $< 0.5$ at.% for the germanide. Although this small amount of carbon may have some stabilizing effect on a certain structure type, the influence of carbon on the formation of the HT-PuAl3 structure is expected to be negligible compared to the effect introduced by Si and Ge in our compounds. The reason is that only a certain amount of Si and Ge leads to the pure phases with the HT-$PuAl_3$ structure, albeit all the samples in the two phase region as well as the $YbAl_3$ samples have

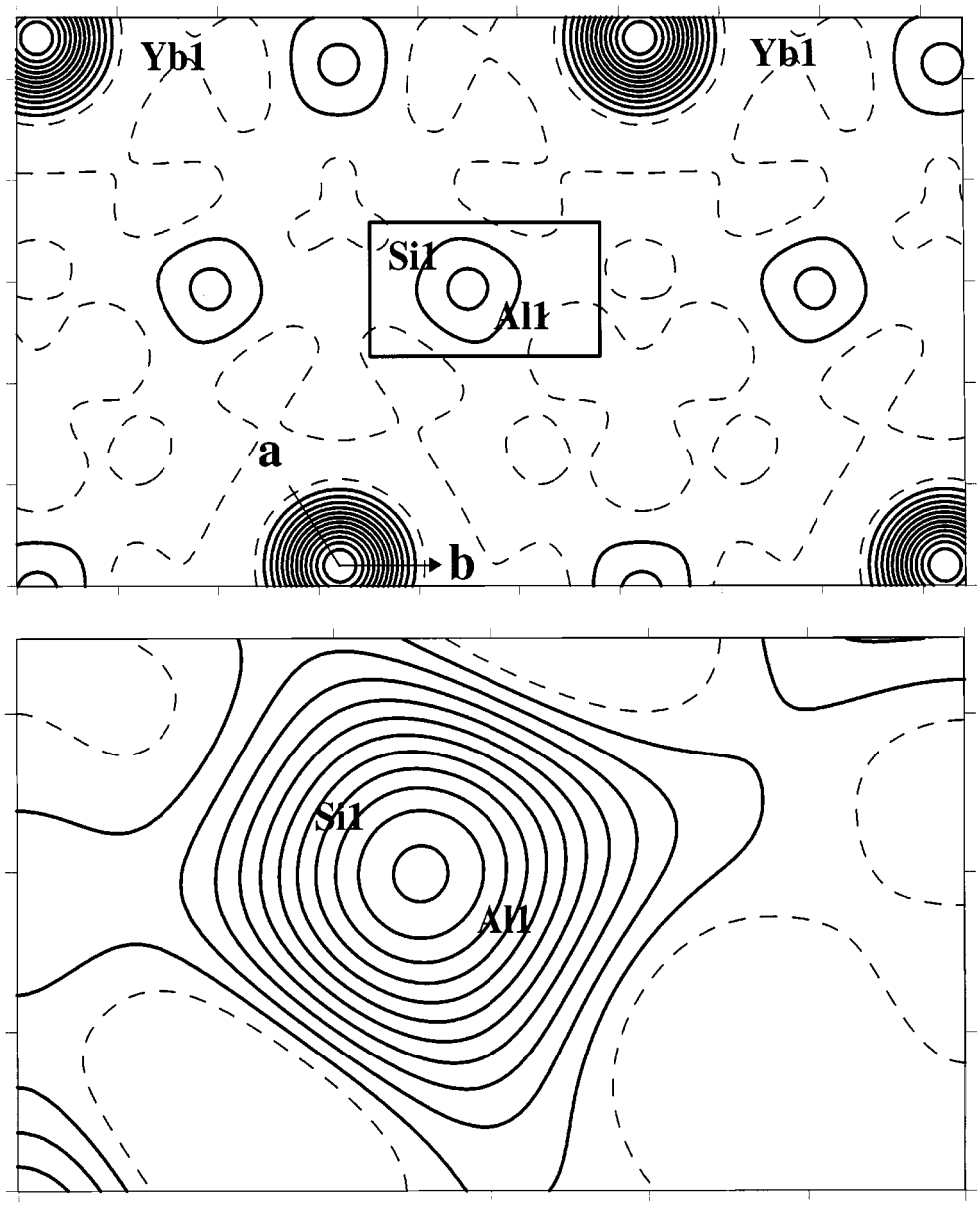


**FIG. 2.** Electron density in the $xy\frac{1}{4}$ plane for $Yb_{1-y}Al_{2.8}Si_{0.2}$ calculated from the X-ray powder diffraction data. Full lines for positive density; dashed lines for zero values. (Upper panel) Fourier map calculated without Al1 and Si1 positions. (Lower panel) Electron-density difference map of the region around the Al1 and Si1 positions marked in the upper panel.

been processed the same way. Additionally, both new phases can also be prepared in a Ta crucible with HF melting without any participation of carbon in the reaction.

The crystal structure of the $YbE_3$ phases can be described topologically as stacking variants of closest packed layers of the composition $YbE_3$. In the case of $YbAl_3$ ($AuCu_3$ structure type), the stacking sequence is … ABC …, while for the germanium- and silicon-containing phases (HT-$PuAl_3$ structure type), the stacking sequence is given by … ABACBC … (Fig. 3). However, the analysis of the interatomic distances shows that only the $YbAl_3$ structure can be interpreted as a closest packing (all distances in the first coordination shell are equal). Replacement of a small amount of aluminum by germanium or silicon leads to the appearance of covalently bonded homoatomic clusters $E_3$ and spreads the interatomic distances over relatively wide ranges. Similar effects were observed in a bonding analysis in some binary compounds of the early transition metals with the triels and tetrels (14).

The magnetic susceptibility of the $Yb_{1-y}Al_{3-x}Si_x$ and $Yb_{1-y}Al_{3-x}Ge_x$ samples was investigated in external

**TABLE 5**
**Atomic Positional and Displacement Parameters for $Yb_{1-y}Al_{2.8}Si_{0.2}$**

| Atom | Site | SOF | $x$ | $y$ | $z$ | $U_{iso}$ (in Å$^2$) |
|---|---|---|---|---|---|---|
| Yb1 | 2*b* | 1 | 0 | 0 | $\frac{1}{4}$ | 0.0047(4) |
| Yb2 | 4*f* | 0.963(3) | $\frac{1}{3}$ | $\frac{2}{3}$ | 0.09213(6) | 0.0064(3) |
| Al1 | 6*h* | 0.83[a] | 0.5188(7) | $2x-1$ | $\frac{1}{4}$ | 0.009(1) |
| Si1 | | 0.17 | 0.537(4) | $2x-1$ | $\frac{1}{4}$ | 0.009 |
| Al2 | 12*k* | 0.985[a] | 0.8325(3) | $2x-1$ | 0.0812(2) | 0.0121(7) |
| Si2 | | 0.015 | 0.8325 | $2x-1$ | 0.0812 | 0.0121 |

[a]Occupancy values were fixed according to the germanide refinement (Table 3).

magnetic fields between 100 Oe and 40 kOe. Relevant results are shown in Fig. 4. Neither magnetic order nor superconductivity was found above 1.8 K. The $\chi(T)$ curves of all substituted samples display the same typical broad maximum as observed for $YbAl_3$ (1, 15). Taking into account some impurities, giving rise to the upturn of $\chi(T)$ below 25 K, the extrapolated values of $\chi$ at helium temperature ($T \to 0$) can be estimated. For $YbAl_3$, $\chi(0) \approx 5.3 \times 10^{-3}$ emu/mol would correspond to an electronic specific heat coefficient $\gamma \approx 390\ \mathrm{mJ\,mol^{-1}\,K^{-2}}$ within the free

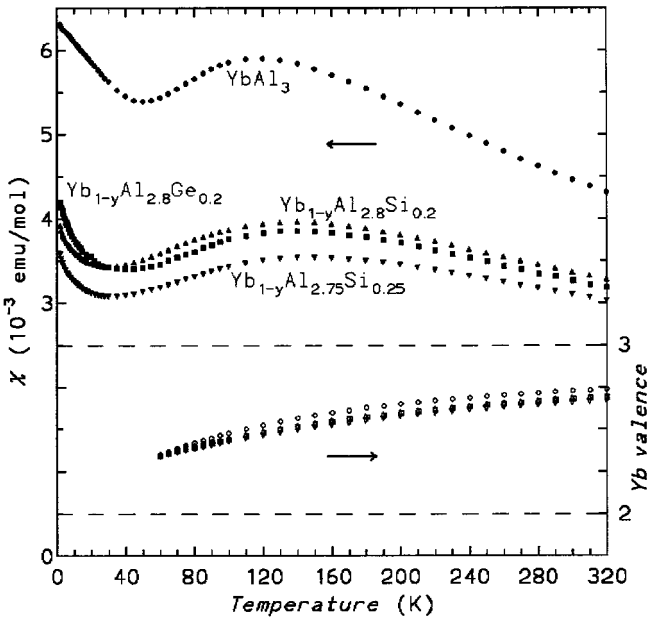


**FIG. 4.** Temperature dependence of the magnetic susceptibility (upper panel) for $Yb_{1-y}Al_{3-x}Si_x$ and $Yb_{1-y}Al_{3-x}Ge_x$ in comparison with that of $YbAl_3$. The curves for $YbAl_3$ and $Yb_{1-y}Al_{2.8}Si_{0.2}$ were measured at an external field of 20 kOe and the other two curves at 10 kOe. The right-hand scale shows the temperature dependence of the Yb valence as calculated from the ICF model (17) (lower panel). Symbols are the open versions of the respective $\chi(T)$ curves.

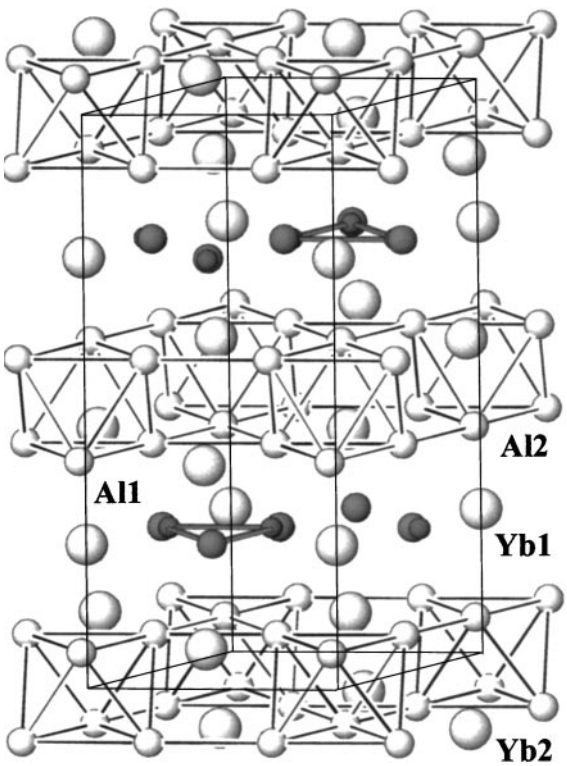


**FIG. 3.** $E_3$ "clusters" and aluminum networks in $Yb_{1-y}Al_{2.8}Si_{0.2}$ and $Yb_{1-y}Al_{2.8}Ge_{0.2}$ structures.

electron gas approximation. However, the value of $\gamma$ found experimentally is much smaller, cf. $\gamma \approx 58\ \mathrm{mJ\,mol^{-1}\,K^{-2}}$ (14). Generally, the values of $\gamma$ and $\chi_0$ do not scale for intermediate valence compounds of ytterbium (3). Substitution of aluminum with $x = 0.2$ Ge or Si leads to a reduction to 65% of the $\chi(0)$ value of the binary phase and the larger Si substitution ($x = 0.25$) reduces $\chi(0)$ further to about 55%. This can be understood by a decrease of the hybridization strength at the Fermi level as a consequence of the covalent bonds in $E_3$ clusters. The maximum of $\chi(T)$ at $T_{max}$ increases from $T_{max} \approx 120$ K for $YbAl_3$ to $T_{max} \approx 140$ K for $Yb_{1-y}Al_{2.8}Si_{0.2}$ and $Yb_{1-y}Al_{2.8}Ge_{0.2}$ and further to $\approx 150$ K for $Yb_{1-y}Al_{2.75}Si_{0.25}$. A similar increase of $T_{max}$ with substitution was also observed in the phase $Yb_{1-x}Sc_xAl_3$ (15). The small substitution of Yb by Sc leads to a strong increase of $T_{max}$. In all three phases, $Yb_{1-x}Sc_xAl_3$, $Yb_{1-y}Al_{2.8}Si_{0.2}$, and $Yb_{1-y}Al_{2.8}Ge_{0.2}$, the increase of $T_{max}$ can be correlated to a decrease of the valence state.

This result is consistent with simple electron counts. Assuming that the electron number in $YbAl_3$ is enough to stabilize the bonding situation (three 5c–4e$^-$ bonded flat $Yb_4Al$ groups per unit cell), as was similarly shown for $ZrGa_3$ (16), additional electrons of silicon (germanium) would be partially used for stabilizing the 3c–2e$^-$ or even 2c–2e$^-$ bonds and would partially make the full occupation

**TABLE 6**
**The Fitted $T_{sf}$ and $T_{ex}$ Values ($T_{ex} = E_{ex}/k_B$) of the ISF Model (Error Margins Are Only the Statistical Error)**

| Sample | $T_{sf}$ (K) | $T_{ex}$ (K) | $\chi(0)$ ($10^6$ emu mol$^{-1}$) | $T_{max}$ (K) |
|---|---|---|---|---|
| $YbAl_3$ | 104(1) | 442(2) | − 157(26) | − 118 |
| $Yb_{1-y}Al_{2.8}Si_{0.2}$ | 170(1) | 621(3) | − 363(17) | − 138 |
| $Yb_{1-y}Al_{2.75}Si_{0.25}$ | 193(2) | 688(4) | − 350(20) | − 148 |
| $Yb_{1-y}Al_{2.8}Ge_{0.2}$ | 168(2) | 620(3) | − 471(20) | − 139 |

of the ytterbium position unnecessary (the number of electrons per formula unit is 12 for $YbAl_3$, 12.13 for $Yb_{0.963}Al_{2.8}Si_{0.2}$, 12.10 for $Yb_{0.948}Al_{2.8}Ge_{0.2}$, and 12.20 for the ideal $YbAl_{2.8}E_{0.2}$ composition).

Above 240 K, the susceptibility can be described by a Curie–Weiss law $\chi = C/(T - \theta_{CW})$. As observed previously, even at this high temperature, $\theta_{CW}$ and $\mu_{eff}$ depend on the temperature range of the fit (5). $\theta_{CW}$ is negative and large ($YbAl_3$: − 280 K; $Yb_{1-y}Al_{2.8}Si_{0.2}$ and $Yb_{1-y}Al_{2.8}Ge_{0.2}$: − 480 K; $Yb_{1-y}Al_{2.75}Si_{0.25}$: − 580 K), while the fitted effective magnetic moments $\mu_{eff}$ are around the value of the free $Yb^{3+}$ ion (4.54 $\mu_B$). A better description of the magnetic behavior above 60 K can be given by the interconfiguration fluctuation (ICF) model by Sales and Wohlleben (17) with two parameters: the energy separation $E_{ex}$ of the $Yb^{2+}$ and the $Yb^{3+}$ configuration and the temperature $T_{sf}$. The fitted values are given in Table 6. From the fit the temperature dependence of the valence of ytterbium can be calculated (see Fig. 4, lower panel). For $YbAl_3$ and the derivatives the valence increases smoothly with temperature from 2.35 at 60 K to 2.75 at 400 K. As in (17) the susceptibility data below 60 K could not be fitted, in spite of the inclusion of a test with a Curie contribution for paramagnetic impurities in the fit. This is due to the presence of a second maximum $\chi(T)$ in $YbAl_3$ at around 15 K (18, 19), which is intrinsic and ascribed to the establishment of Fermi liquid coherence (19). For all fits a small $\chi(0)$ had to be included. The values $T_{sf}$ and $E_{ex}/k_B$ and for the $x = 0.2$ samples are the same for the Ge and the Si sample, but they are both about 50% larger than those for $YbAl_3$. Consequently, the Yb valence of the derived phases ($x = 0.2$) is about 0.05 less than that in $YbAl_3$ at 400 K.

The resistivity of the polycrystalline samples (Fig. 5) behaves similarly to that of $YbAl_3$. The large residual resistivity of our samples is—for the most part—probably due to microcracks and grain boundaries in contrast to the single-crystal data recently published for $YbAl_3$ (18). Since the contribution of grain boundaries and cracks to $\rho_0 = \rho(T \to 0)$ is unknown, nothing can be said about the influence of point defects. Such kinds of defects certainly exist in the ternary intermetallic compounds, but an investigation of the defects requires the preparation of sufficiently large single crystals for transport measurements. Observing now only $\rho(300\,K)$-$\rho_0$, a significantly larger value is observed for $Yb_{1-y}Al_{2.8}Ge_{0.2}$ (117 μΩ cm) than for $Yb_{1-y}Al_{2.8}Si_{0.2}$ (39 μΩ cm). This is quite surprising since the magnetic properties of both samples are very similar. Ebihara *et al.* (14) report a $\rho(300\,K) - \rho_0$ value of 30 μΩ cm for $YbAl_3$, which is not much smaller than that for $Yb_{1-y}Al_{2.8}Si_{0.2}$. The S-shape of all $\rho(T) - \rho_0$ curves is characteristic for valence fluctuation compounds.

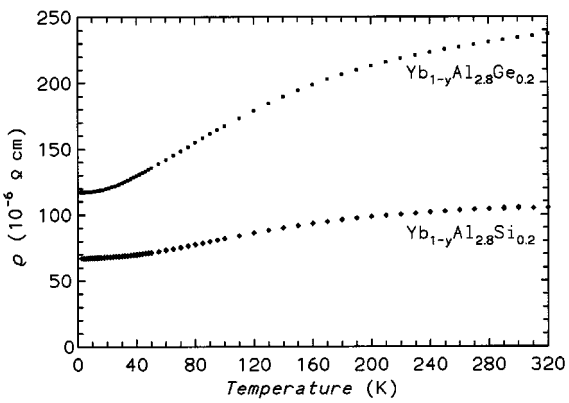


**FIG. 5.** Temperature dependence of the electrical resistivity of $Yb_{1-y}Al_{2.8}Si_{0.2}$ and $Yb_{1-y}Al_{2.8}Ge_{0.2}$ compounds.

## ACKNOWLEDGMENTS

This project was supported by the Fonds der Chemischen Industrie. J.T.Z. is indebted to the support by the National Science Fund for Distinguished Young Scholars from the NNSF of China and to the Max-Planck-Gesellschaft for a research fellowship. We also thank Dr. H. Borrmann and Dr. R. Cardoso for the XRD data collection and Mrs. U. Schmidt for performing the chemical analysis.

## REFERENCES

1. N. B. Brandt and V. V. Moshchalkov, *Adv. Phys.* **33,** 373 (1984).
2. Z. Fisk and M. B. Maple, *J. Alloys Compd.* **183,** 303 (1992).
3. J. P. C. Klaasse, F. R. de Boer, and P. F. de Châtel, *Physica B* **106,** 178 (1981).
4. R. Eggenhöffner, *Nuovo Cimento D* **15,** 519 (1993).
5. A. Hiess, J. X. Boucherle, F. Givord, J. Schweizer, E. Lelièvre-Berna, F. Tasset, B. Gillon, and P. C. Canfield, *J. Phys. Condens. Matter* **12,** 829 (2000).
6. A. Iandelli and A. Palenzona, *J. Less-Common Met.* **29,** 293 (1972).
7. J. T. Zhao and E. Parthé, *Acta Crystallogr. C* **47,** 1 (1991).
8. O. S. Zarechnyuk, A. A. Muravyeva, and E. I. Gladyshevsky, *Dopov. Akad. Nauk Ukr-RSR A* 753 (1970).
9. J. T. Zhao, H. Borrman, S. Paschen, W. Schnelle, and Yu. Grin, *Z. Kristallogr. New Cryst. Struct* **215,** 200 (2000).
10. C. Kranenberg, D. Johrendt, and A. Mewis, *Z. Anorg. Allg. Chem.* **625,** 1787 (1999).

11. J. T. Zhao, W. Schnelle, and Yu. Grin, *Z. Krist. NCS*, in press.
12. J. T. Zhao, W. Schnelle, and Yu. Grin, to be submitted.
13. L. G. Akselrud, P. Y. Zavalii, Yu. Grin, V. K. Pecharsky, B. Baumgartner, and E. Wölfel, *Mater. Sci. Forum* **133–136,** 335 (1993).
14. T. Ebihara, S. Uji, C. Terakura, T. Terashima, E. Yamamoto, Y. Haga, Y. Inada, and Y. Onuki, *Physica B* **281 & 282,** 754 (2000).
15. R. E. Majewski, A. S. Edelstein, A. T. Aldred, and A. E. Dwight, *J. Appl. Phys.* **49,** 2096 (1978).
16. Yu. Grin, U. Wedig, and H. G. von Schnering, *in* "12th Int. Conf. on Solid Compounds of Transition Elements. Abstracts. Saint-Malo, France," p. O–35. 1997.
17. B. C. Sales and D. K. Wohlleben, *Phys. Rev. Lett.* **35,** 1240 (1975).
18. A. Hiess, J. X. Boucherle, F. Givord, and P. C. Canfield, *J. Alloys Compd.* **224,** 33 (1995).
19. J. M. Lawrence, T. Ebihara, P. S. Riseborough, C. H. Booth, M. F. Hundley, P. G. Pagliuso, J. L. Sarrao, J. D. Thompson, M. H. Jung, A. H. Lacerda, and G. H. Kwei, *Cond-mat*/0107638, 31 July 2001.